NUMERICAL STUDY OF THE EFFECT OF PERIODIC WAKE ON FILM COOLING EFFECTIVENESS ON A PLATE

Liuliu SHI [1,2*], ***Haobo FAN*** [1,2], ***Eryun CHEN*** [1,2]

[1] School of Energy and Power Engineering, University of Shanghai for Science and Technology, Shanghai 200093, China

[2] Shanghai Key Laboratory of Multiphase Flow and Heat Transfer in Power Engineering, Shanghai 200093, China

[*] Corresponding author; e-mail: shiliuliu@usst.edu.cn

The research presented in this paper is devoted to exploring the influence of upstream periodic wake on the film cooling effectiveness on a downstream plate. This investigation is carried out through rigorous numerical simulations utilizing a dedicated simulation model. The model was developed to examine the impact of upstream periodic wake on film cooling performance across varying blowing ratios (M = 0.3, 0.5, and 1.0) and wake sweeping frequencies (10 Hz, 20 Hz, and 40 Hz). Comparative analyses are conducted with a baseline scenario involving a constant jet without wake. The objective of these analyses is to provide a deeper understanding of the mechanisms through which upstream wake influences film cooling performance, ultimately shedding light on the flow characteristics and cooling effectiveness of film cooling under sweeping wakes.

Keywords: *gas turbine; film cooling; wake; blowing ratio*

1. Introduction

Gas turbines are extensively employed in power generation, marine, and aeroengines due to their outstanding efficiency. In pursuit of increased turbine efficiency, higher turbine inlet temperatures are adopted to elevate the thermal efficiency. This results in a substantial rise in the gas temperature entering the turbine stages [1], surpassing the operational limits of most substrate materials. In addition to the advancement of novel heat-resistant materials, turbine blade cooling technology assumes a pivotal role in enabling the stable operation of turbine blades under such severe environment. Notably, film cooling stands out as a highly efficient and widely adopted method for blade cooling.

In the stages of a turbine, the interaction between rotors and stators results in periodic wake disturbances from upstream blades impacting downstream blades, consequently affecting film cooling performance [2-4]. Research by Schulte and Hodson [5] has shown that using cylindrical rods to simulate the interfering wake can elicit a similar effect to the actual wake. Ou and Han [6] conducted experimental investigations, indicating that higher blowing ratios and increased Strouhal numbers lead to reduced cooling efficiency on the pressure side of the blade. Du et al. [7] similarly observed a reduction in film cooling performance on both sides of the blade at a blowing ratio of 0.8. Additionally, Heidmann and Lucci [8] noted the pressure surface to be more sensitive to upstream wake effects than the suction surface.

Womack et al. [9] and Golsen et al. [10] found that at low blowing ratios, increasing the Strouhal number reduces cooling efficiency. Conversely, at high blowing ratios, the wake enhances the capacity of the coolant jet to reattach to the wall and expand laterally, thereby amplifying film cooling effectiveness. Colban et al. [11] observed that the coolant jet tends to lift at the outlet of the cooling hole, resulting in reduced cooling effectiveness immediately downstream of the hole. These findings align with those of Polanka et al. [12] and Zhang et al. [13], suggesting that the turbulence induced by the upstream wake heightens mixing in the mainstream, guiding the coolant jet to reattach to the wall. Gomes and Niehuis [14] indicated that the wake intensifies turbulence in the separation zone along the pressure surface of the blade, ultimately reinforcing film cooling effectiveness. Gao et al. [15] analyzed the effect of the relative position of the wake on film cooling performance by varying the upstream position of the wake generator. Similarly, Li et al. [16] investigated the impact of unsteady upstream wake and blade trailing edge jets on film cooling effectiveness using pressure-sensitive paint, demonstrating a reduction in film cooling effectiveness, but an enhancement in effectiveness with the addition of a trailing edge jet.

Current research underscores that, under varied experimental conditions, these periodic wake disturbances may either enhance or diminish film cooling effectiveness. Accordingly, comprehending these complexities is vital for optimizing film cooling strategies in gas turbine applications. To this end, a numerical simulation model was established in this study to investigate the impact of upstream periodic wake on film cooling performance under varying blowing ratios (M = 0.3, 0.5, and 1.0) and wake sweeping frequencies (10 Hz, 20 Hz, and 40 Hz), with experimental data [17] laying the groundwork for numerical simulations. Comparisons were made against a baseline scenario of constant jet without wake. These analyses aimed to provide insight into the mechanisms through which upstream wake influences film cooling performance, ultimately elucidating the flow characteristics and cooling effectiveness of film cooling under sweeping wakes.

2. Numerical methods

2.1. Governing equations

The flow is governed by the three-dimensional continuity, momentum, and energy conservation equations, which is defined as follows:

$$\frac{\partial \rho}{\partial t} + \nabla \cdot (\rho \boldsymbol{v}) = 0 \tag{1}$$

where ρ is the background density of the stratified flow and $\boldsymbol{v}$ is the velocity vector.

$$\frac{\partial}{\partial t}(\rho \boldsymbol{v}) + \nabla \cdot (\rho \boldsymbol{v}\boldsymbol{v}) = -\nabla p + \nabla \cdot (\boldsymbol{\tau}) + \rho \boldsymbol{g} \tag{2}$$

Where $\boldsymbol{\tau}$ is the shear stress.

$$\frac{\partial}{\partial t}(\rho T) = -\nabla \cdot (\rho \boldsymbol{v} T) + \nabla \cdot (\frac{k}{c} \nabla (T)) \tag{3}$$

where T is the temperature, k is the thermal conductivity, and c is the specific heat

capacity.

2.2. Numerical setup

The computational domain and grid are shown in Fig. 1. A cylindrical rod with the same diameter D of the film cooling hole is used as a wake generator, and it is placed at 11.5D upstream of the film cooling hole.

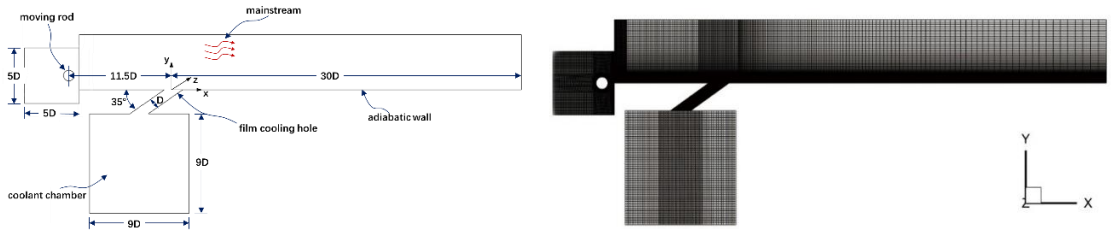

(a) (b)

Fig. 1. Schematic diagram of the computational domain and grid

The rod moves at different speeds in the Y direction to generate wake with different sweeping frequencies. To meet the requirement of periodic sweeping, the upper and lower boundaries of the wake region are set as periodic boundary conditions. The wake sweeping frequency is set at 10 HZ, 20 HZ, and 40 HZ by adjusting the moving speed of the wake generator. The incompressible air is specified as the working fluid of both the mainstream and the coolant. The mainstream velocity u_∞ is set at 8 m/s and the mainstream temperature T_∞ is set at 273 K. The bottom of the coolant chamber is designated as the inlet of the cooling flow and the temperature of the coolant jet is set at 300 K. The blowing ratio M varies as the massflow rate of the coolant jet changes. The flat bottom wall of the mainstream domain is an adiabatic non-slip wall. The specific parameters considered in present study is shown in Table 1. More details about the experimental setting refer to Coulthard S M et al. [20]. The numerical simulations have been carried out by using ANSYS FLUENT.

Table 1. experimental settings of the present study

blowing ratio	wake frequency (Hz)		
M=0.3	10	20	40
M=0.5	10	20	40
M=1.0	10	20	40

2.3. Parameter Definition

The blowing ratio M is defined as:

$$\mathrm{M} = \frac{\rho_c \mathrm{V_c}}{\rho_\infty \mathrm{V_\infty}} \tag{4}$$

where ρ_c and ρ_∞ are the jet and main stream densities, and $\mathrm{V_c}$ and $\mathrm{V_\infty}$ are the cooling jet velocity at the exit of the film cooling hole and mainstream velocity, respectively.

The adiabatic film cooling efficiency η is defined as:

$$\eta = \frac{T_{aw} - T_\infty}{T_{jet} - T_\infty} \tag{5}$$

Where T_{aw} is the adiabatic wall surface temperature, T_{jet} is the jet temperature and T_∞ is

the main flow temperature.

2.4. Grid independence study

In order to conduct the grid independence analysis, four sets of grids with varying sizes were chosen, each comprising approximately 1.5 million, 2 million, 2.6 million, and 4.3 million grid cells. The results of film cooling effectiveness of these grid set along the centerline are presented in Fig. 2. The results reveal discernible discrepancies at the cooling hole outlets with increasing grid numbers. Notably, upon reaching 2 million grids or more, no further consequential variations in the calculated outcomes are observed. Consequently, the grid set comprising approximately 2 million grids is selected for subsequent numerical simulations.

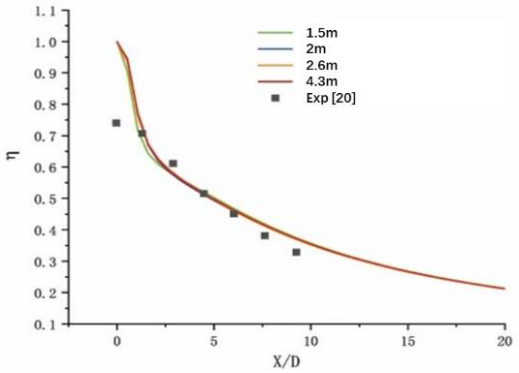

Fig. 2. Streamwise distribution of the film cooling effectiveness with different grids

2.5. Turbulence model independence study

Four turbulence models (i.e., Standard k-ε, RNG k-ε, Realizable k-ε and SST-ω) and three near-wall functions (i.e., standard wall functions, non-equilibrium wall functions and enhanced wall treatment) are selected for comparison with the experimental results [20]. The resultant film cooling effectiveness are given in Fig. 3, the RNG k-ε turbulence model with non-equilibrium wall function shows best performance and is chosen for numerical simulations in this paper.

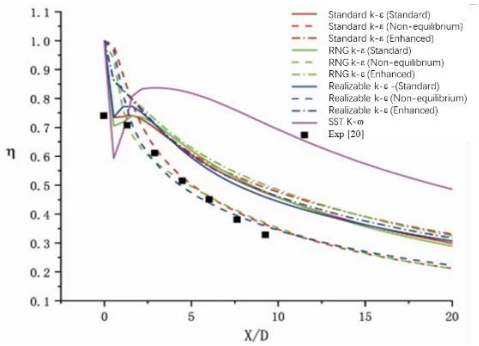

Fig. 3. Streamwise distribution of the film cooling effectiveness with different turbulence models

3. Results and Discussion

3.1. Influence of the sweeping wake on film cooling performance at M = 0.3

The instantaneous snapshots of contours of vorticity and temperature are shown in Fig.4, which gives a preliminary impression on how the upstream wake impact on downstream film cooling performance. The coolant flow is ejected from the film cooling hole, and covers the downstream area and gives protection to the endwall in case without upstream wake. However, as can be seen at M=0.3, large-scale vortices are shed from upstream moving rod, and interact with the coolant flow ejected from the cooling hole. The stable coverage of the coolant flow on downstream plate was destroyed. With the increase in the sweeping frequency of the moving rod, the mixing of the main flow and the coolant flow increases. The film cooling effectiveness decreases apparently, however, the streamwise extend of the coolant flow increases.

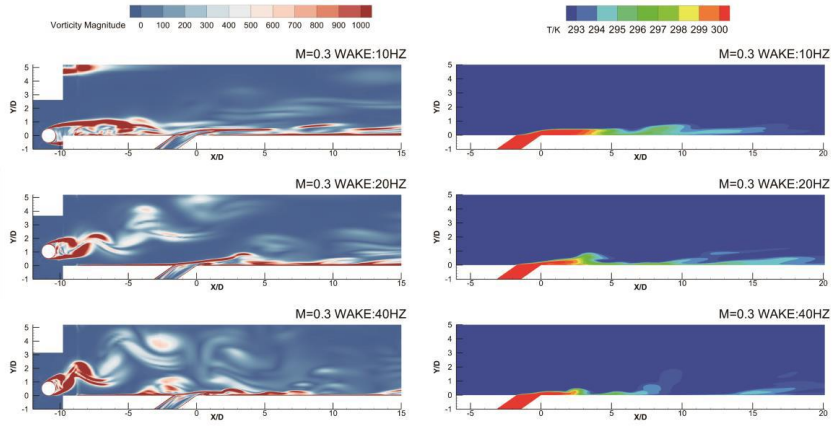

Fig. 4. Instantaneous contours of vorticity and temperature in Z=0

The streamwise distributions of laterally-averaged film efficiency effectiveness are given in Fig.5. It is observed that under the influence of upstream wake, the film cooling effectiveness increases, among which the largest efficiency improvement is for the 20 HZ sweeping frequency condition, and the efficiency is nearly doubled.

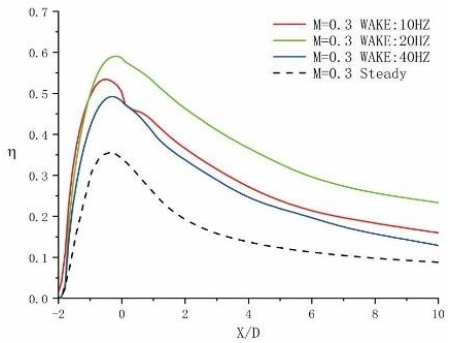

Fig. 5. Streamwise distributions of laterally-averaged film cooling effectiveness

The overall averaged film cooling effectiveness in the streamwise range $-1 \leq x/D \leq 10$ is given in Table. 2. Compare to the steady case that without the influence of the moving rod, the film cooling effectiveness in cases with the moving rod all increase dramatically. It increases from 0.1828 to 0.2933 for case with sweeping frequency of 10HZ, and it reaches a maximum in case with sweeping frequency of 20HZ, which increase from 0.1828 to 0.3764

with an increment of nearly 106%. Further increase in the sweeping frequency results in a decrease in the increment with sweeping frequency of 40HZ.

Table 2. Overall averaged film cooling effectiveness at various blowing ratios

M	Steady	10 HZ	20 HZ	40 HZ
0.3	0.1828	0.2933	0.3764	0.2675
0.5	0.2095	0.3234	0.3406	0.3078
1.0	0.1172	0.1108	0.0977	0.1093

Fig. 6 displays the contours of the time-averaged film cooling effectiveness on the plate. This demonstrates why the film cooling effectiveness becomes stronger in the presence of the wake. The figure indicates that under different operating conditions with wake, the width of the cooling film in the spanwise direction is significantly larger compared to cases without wake. This shows that the wake expands the spanwise coverage area of the cooling film, leading to a substantial improvement in film cooling efficiency. Additionally, the streamwise extent of the cooling film also increases at 10Hz and 20Hz.

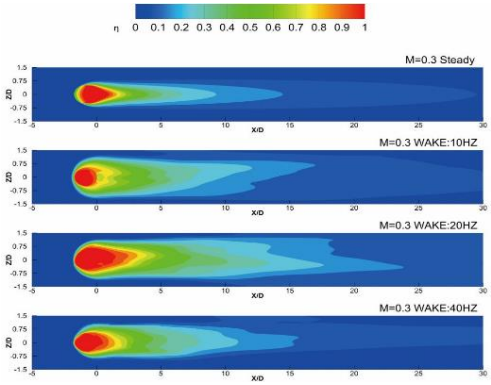

Fig. 6 Contours of time-averaged film cooling effectiveness on the plate

In Fig. 7, the temperature contours at three different positions along the streamwise direction are shown. The figures indicate that the incoming wake significantly alters the structure of the cooling jet. At the position X=D, the coverage area of the cooling film increases from D to 2D, and the height of the jet center decreases due to the influence of the wake vortex. This same effect is observed at positions X=5D and 10D. Overall, at a blowing ratio of M=0.3, the wake has a favorable effect on the film cooling efficiency.

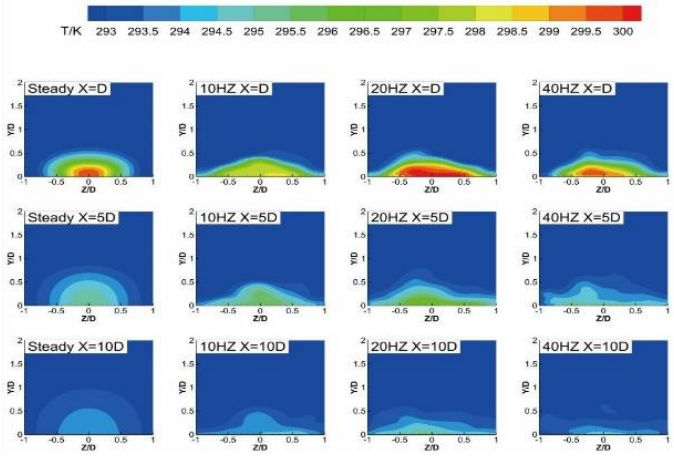

Fig. 7 Contours of temperature at different streamwise locations

3.2. Influence of the sweeping wake on film cooling performance at M = 0.5

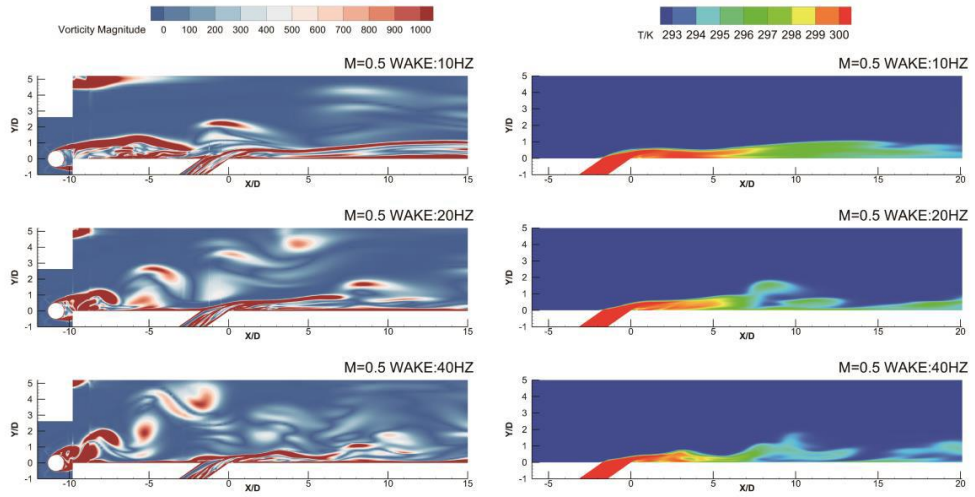

Fig. 8. Instantaneous contours of vorticity and temperature in Z=0

In Fig. 8, the vorticity and temperature contours are shown at a blowing ratio of M=0.5. Compared to a blowing ratio of M=0.3, the cooling film on the plate is more stable due to the higher blowing ratio. When the wake frequency is 10Hz, the coverage range of the cooling film in the streamwise direction increases from 10D to 20D compared to the blowing ratio M=0.3. The coverage range of the cooling film also doubles at frequencies of 20Hz and 40Hz. However, as the wake frequency increases, the interaction between the wake and the cooling film leads to the destruction of the stable film coverage, resulting in a decrease in the cooling film's coverage effect.

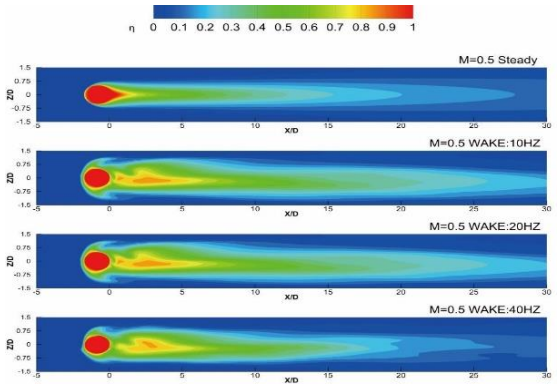

Fig. 9 Contours of time-averaged film cooling effectiveness on the plate

Fig. 9 displays the contours of the time-averaged film cooling effectiveness on the plate. The film cooling coverage is wider at the outlet of the cooling hole due to the wake's influence, but it becomes narrower behind the outlet, with a coverage area similar to that without wake interference. Fig.10, showing the laterally averaged film cooling effectiveness, also indicates a significant decrease in efficiency behind the cooling hole. Notably, except for the 20Hz wake frequency, the film cooling effectiveness is almost the same as that without wake interference. The statistical results in Table 2 reveal that at a blowing ratio (M) of 0.5, the film cooling effectiveness with wake interference improves by approximately 50% compared to that without wake interference.

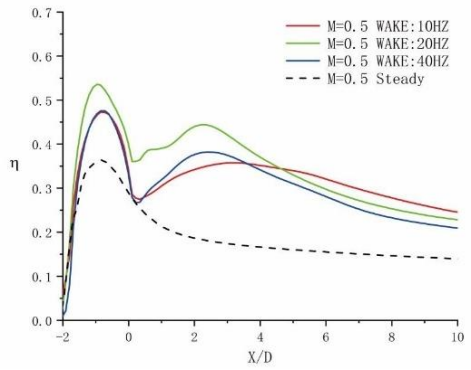

Fig. 10. Streamwise distributions of laterally-averaged film cooling effectiveness

Fig. 11 displays temperature contours at three different positions along the streamwise direction. At a blowing ratio of M=0.5, the wake has a positive impact on the film cooling efficiency on the plate. While the cooling effect is slightly lower compared to that of M=0.3, the film structure's stability is enhanced. The coverage within the 10D range is improved despite the disturbance caused by the wake vortex, making it superior to the M=0.3 condition.

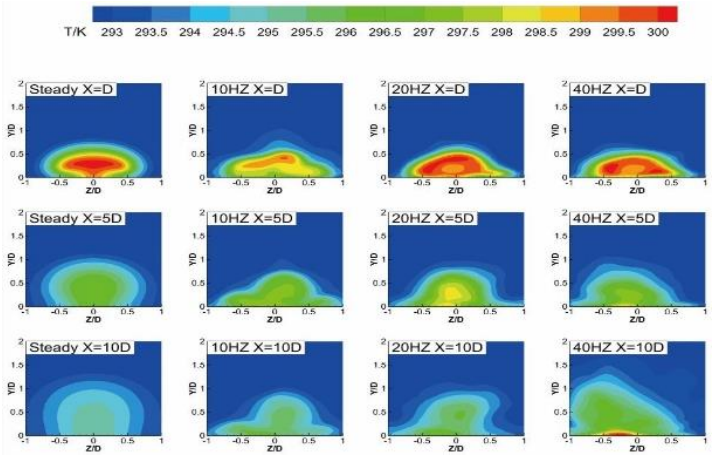

Fig. 11. Contours of temperature at different streamwise locations

3.3. Influence of the sweeping wake on film cooling performance at M = 1.0

In Fig. 12, the contours of vorticity and temperature are depicted at a blowing ratio of M=1.0. When the blowing ratio increases to 1.0, the velocity of the cooling jet at the outlet of the film hole increases, causing the cooling jet to rise and weakening the local cooling effect. As a result of the increased momentum of the cooling jet, the interaction between the wake and the cooling flow weakens, delaying the damage to the flat plate. This phenomenon occurs at X=3D under the blowing ratio M=0.3, at X=8D under M=0.5, and only at X=20D when the wake frequency reaches 40Hz under M=1.0.

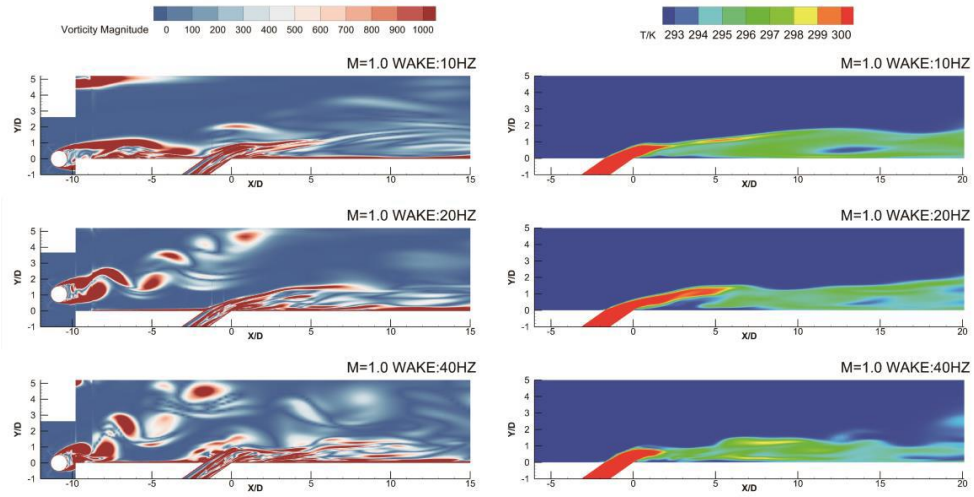

Fig. 12. Instantaneous contours of vorticity and temperature in Z=0

In Fig. 13, we can see that the averaged film cooling effectiveness behind the film hole is lower under wake disturbance compared to no-wake condition. However, this effectiveness gradually increases with distance and eventually surpasses the cooling efficiency under no-wake condition. When comparing the efficiency curves behind the film hole at blowing ratios M=0.3 and M=0.5, we notice that the change in efficiency behind the film hole is significantly influenced by the blowing ratio. In general, the film cooling effectiveness is higher under the disturbance of incoming wake compared to the condition without wake disturbance.

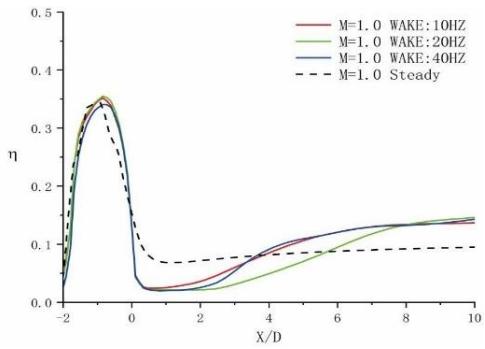

Fig. 13. streamwise distributions of laterally-averaged film cooling effectiveness

Fig. 14 depicts the contours of the time-averaged film cooling effectiveness on the plate. It is noteworthy that an increase in the blowing ratio to 1.0 results in the inability of the cooling jet to affect the plate surface within the 5D range behind the film hole, owing to the influence of the incoming wake. Additionally, at 5D from the outlet, the cooling jet reattaches to the plate, exhibiting a broader coverage width compared to the steady state. The overall averaged film cooling effectiveness, as presented in Table 2, denotes a decrease in cooling efficiency at M=1.0 under the influence of the sweeping wake.

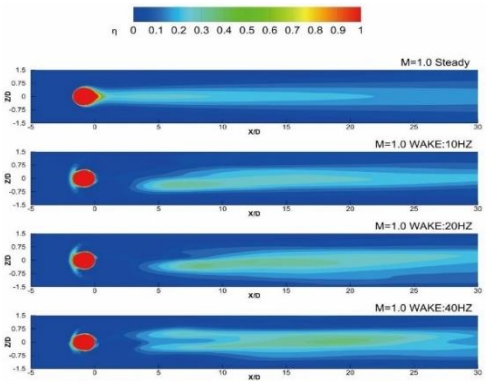

Fig. 14 Contours of time-averaged film cooling effectiveness on the plate

As shown in Fig. 15, at X=D, compared to the condition without upstream wake influence, the overall distribution of the cooling jet with upstream wake disturbance is not significantly different. At the X=5D section, the vertical velocity of the jet decreases, the height of the jet decreases, and it reattaches to the plate. At X=10D, the jet height further decreases, and the spanwise coverage area increases. Due to the larger jet flowrate under at M=1.0, the streamwise coverage of the jet is longer.

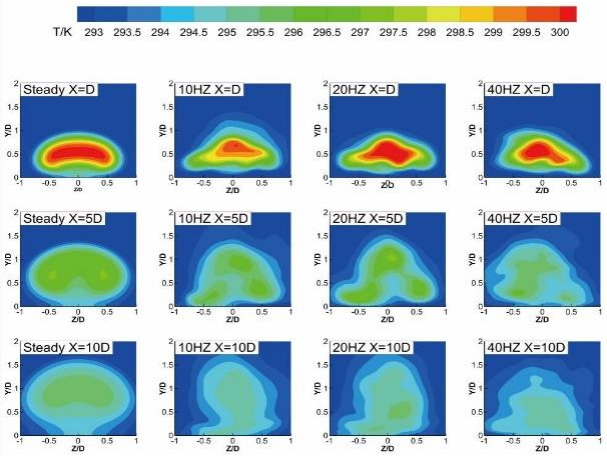

Fig. 15. Contours of temperature at different streamwise locations

4. Conclusions

This paper extensively explores the application of the flat plate film cooling model and integrates cylindrical rods upstream of the flat plate to represent distinct sweeping wakes. These wakes are carefully examined to assess their impact on the cooling effectiveness of the cooling film. The findings demonstrate that the wake vortex plays a crucial role in impeding the formation of the reverse rotating vortex pair of the jet. This phenomenon leads to an augmented spreading distribution of the cooling film and a noteworthy reduction in the height of the center of the jet, ultimately enhancing the cooling capability of the cooling film. Furthermore, detailed observations reveal that the structural integrity of the jet is compromised under low blowing ratios, resulting in the tendency of the cooling film to drift away in the middle and back sections. Conversely, the study highlights the wake's influential role in intensifying the vortex developed by the mainstream around the jet at high blowing ratios, facilitating the intrusion of the mainstream between the jet and the plate surface, consequently diminishing the cooling effectiveness of the cooling film.

Acknowledgment

We acknowledge the financial support from the National Natural Science Foundation of China (12172227).

Nomenclature

D	diameter of the hole, mm		Greek symbols
M	blowing ratio	ρ_c	coolant density, kg/m^3
T_{aw}	adiabatic wall surface temperature, K	ρ_∞	mainstream density, kg/m^3
T_{jet}	jet temperature, K	η	adiabatic film cooling efficiency
T_∞	main flow temperature, K		
u_c	coolant velocity, m/s		
u_∞	mainstream velocity, m/s		
x	Streamwise coordinate		
y	vertical coordinate		
z	spanwise coordinate		

References

[1] Zhang J, et al. Recent advances in film cooling enhancement: A review [J]. Chinese Journal of Aeronautics, 2020, 33(4).

[2] Huo D C, Fang H L, Gao J, Liao Y N, Jiang Z Y. Unsteady vane-rotor secondary flow interaction of the endwall region in a 1.5-stage variable-geometry turbine. Energy. 2024: 133027.

[3] Wang T Y, Xuan Y M, Han X S. The effects of stator-rotor interaction on unsteady characteristics of turbine tip leakage flow. Aerospace Science and Technology, 2023, 141: 108544.

[4] Chen D W, Zhu H R, Liu C L, Li H T, Li B R, Zhou D E. Combined effects of unsteady wake and free-stream turbulence on turbine blade film cooling with laid-back fan-shaped holes using PSP technique. International Journal of Heat and Mass Transfer, 2019, 133: 382-392.

[5] Schulte V, Hodson H P. Unsteady wake-induced boundary layer transition in high lift LP turbines [J]. ASME Journal of Turbomachinery, 1998, 120(1): 28-35.

[6] Ou S, Han J C. Unsteady wake over a linear turbine blade cascade with air and CO2 film injection: part-2 effect on film effectiveness and heat transfer distribution [J]. ASME Journal of Turbomachiner, 1994, 116(10):730-737.

[7] Du H, Ekkad S V, Han J C, et al. Effect of unsteady wake with trailing edge coolant ejection on film cooling performance for a gas turbine blade [J]. ASME Journal of Heat Transfer, 1999, 121(6): 448-455.

[8] Heidmann J D, Lucci B L. An experimental study of the effect of wake passing on turbine blade film cooling [R]. ASME Paper 97-GT-255, 1997.

[9] Womack, K. M., Volino, R. J., and Schultz, M. P. Measurements in film cooling flows with periodic wakes [J]. ASME Journal of Turbomachinery, 2008, 130: 041008-1-13.

[10] Golsen M J, Tran N V, Ricklick M A, et al. Interaction of rotational wakes and coolant film in a sector annular duct [R]. ASME Paper GT2011-46465, 2011.

[11] Colban W, Gratton A, and Thole K. Heat transfer and film-cooling measurements on a stator vane with fan-shaped cooling holes [J]. ASME Journal of Turbomachinery, 2006, 128: 53-61.

[12] Polanka M, Ethridge M, Cutbirth J, et al. Effects of showerhead injection on film-cooling effectiveness for a downstream row of holes [R]. ASME Paper 2000-GT-240, 2000.

[13] Zhang L., Moon H. Turbine blade film cooling study effects of film hole location on the pressure side [R]. ASME Paper GT2007-27546, 2007.

[14] Gomes R A, Niehuis R. Film cooling effectiveness measurements with periodic unsteady inflow on highly loaded blades with main flow separation [J]. ASME Journal of Turbomachinery, 2011, 133: 021019-1-11.

[15] Gao Z H, Narzary D P, Han J C. Film-cooling on a gas turbine blade pressure side or suction side with compound angle-shaped holes [J]. ASME Journal of Turbomachinery, 2009, 131: 011019-1-11.

[16] Li S J, Rallabandi A P, Han J C. Influence of unsteady wake with trailing edge coolant ejection on turbine blade film cooling [J]. ASME Journal of Turbomachinery, 2012, 134: 061026-1-9.

[17] Coulthard S M, Volino R J, Flack K A. Effect of Jet Pulsing on Film Cooling: Part 1—Effectiveness and Flowfield Temperature Results [C]. ASME Turbo Expo: Power for Land, Sea, and Air. 2006.

Paper submitted: 14 September 2024

Paper revised: 08 November 2024

Paper accepted: 14 December 2024